

Orally efficacious thrombin inhibitors with cyanofluorophenylacetamide as the P2 motif

Kevin D. Kreutter, Tianbao Lu, Lily Lee, Edward C. Giardino, Sharmila Patel, Hui Huang, Guozhang Xu, Mark Fitzgerald, Barbara J. Haertlein, Venkatraman Mohan, Carl Crysler, Stephen Eisennagel, Malini Dasgupta, Martin McMillan, John C. Spurlino, Norman D. Huebert, Bruce E. Maryanoff, Bruce E. Tomczuk, Bruce P. Damiano and Mark R. Player*

Johnson & Johnson Pharmaceutical Research & Development, Welsh & McKean Roads, Spring House, PA 19477, USA

Received 11 February 2008; accepted 31 March 2008

Available online 8 April 2008

Abstract—2-Cyano-6-fluorophenylacetamide was explored as a novel P2 scaffold in the design of thrombin inhibitors. Optimization around this structural motif culminated in **14**, which is a potent thrombin inhibitor ($K_i = 1.2$ nM) that exhibits robust efficacy in canine anticoagulation and thrombosis models upon oral administration.

© 2008 Elsevier Ltd. All rights reserved.

Venous thromboembolism (VTE) and atrial fibrillation (AF) account for approximately 100,000 deaths per year in the U.S. VTE involves the formation of a deep venous thrombus which may dislodge and move to the pulmonary artery as a pulmonary embolus, and AF can induce thrombus formation in the heart leading to strokes.¹ VTE and AF-induced stroke are currently treated with heparin derivatives, which require subcutaneous delivery, and warfarin, which requires dose titration to minimize bleeding complications.²

Since the serine protease thrombin catalyzes the conversion of soluble fibrinogen to insoluble fibrin in the clotting cascade, it is widely believed that an oral thrombin inhibitor could provide a new standard of care in anticoagulation therapy. Early efforts at thrombin inhibitor design frequently employed a highly basic P1 moiety such as guanidine ($pK_a \sim 13$), but these usually suffered from poor pharmacokinetics (PK).³ Strategies to improve PK include the use of a prodrug-masked P1 (e.g., ximelagatran⁴ and dabigatran etexilate⁵) or a weakly basic or nonbasic P1 isostere.⁶

The weakly basic P1 oxyguanidine ($pK_a \sim 7$), when combined with a P2 phenyl scaffold (e.g., **1**; Fig. 1), gave robust PK in dogs ($F = 73\%$; iv $t_{1/2} = 4.4$ h) along with good in vitro potency ($K_i = 4.0$ nM).⁷ However, the concentration of **1** required to double the activated partial thromboplastin time (aPTT)⁸ in human plasma, an in vitro measure of an anticoagulant's potency, was relatively high ($2 \times \text{aPTT} = 7.9$ μM), presumably in part due to $>98\%$ plasma protein binding.⁷ By contrast,

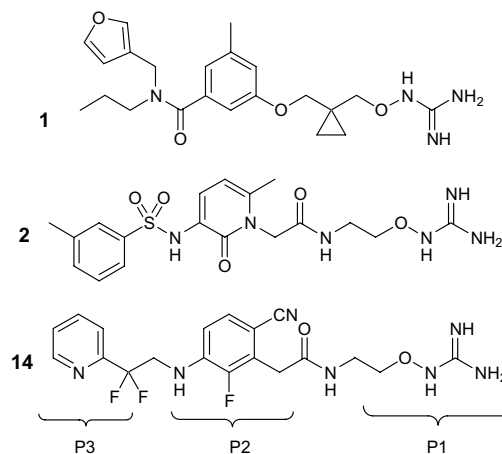


Figure 1. Oxyguanidine-containing thrombin inhibitors.

Keywords: Thrombin inhibitor; Trypsin; Serine protease; Anticoagulant.

* Corresponding author. Tel.: +1 610 458 6980; fax: +1 610 458 8258; e-mail: mplayer@prdu.jnj.com

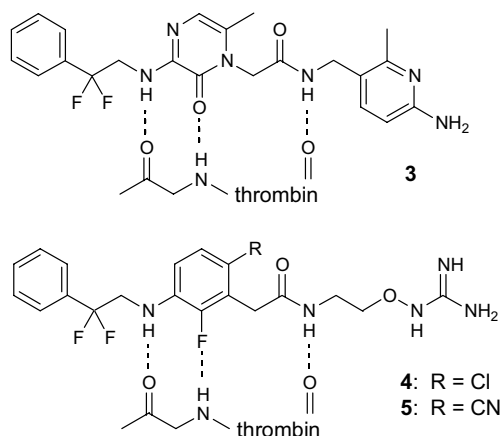


Figure 2. Fluorophenyl compounds **4–5** as H-bond acceptors isosteric with pyrazinone **3**.

while pyridinone-based **2**⁹ displayed an improved $2 \times$ aPTT value of $0.23 \mu\text{M}$ and improved efficacy over **1** (data not shown), it had only modest oral bioavailability (dog $F = 24\%$; rat $F = 6\%$).⁹

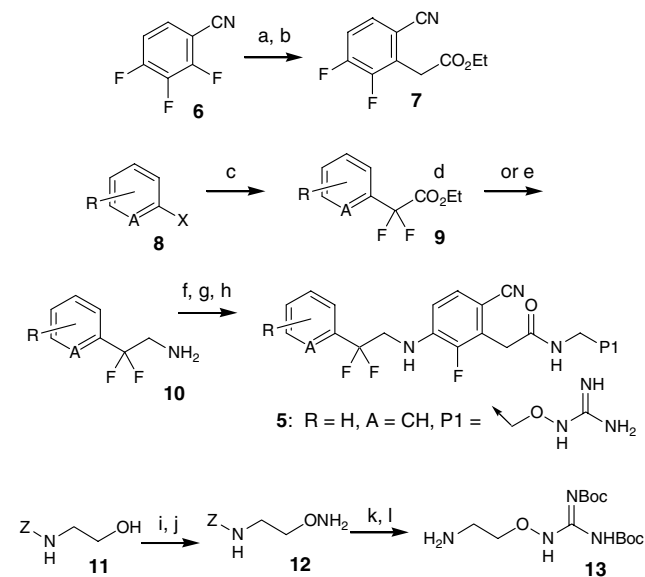
Here we report on a novel 2-cyano-6-fluorophenylacetamide series that led to **14**, a molecule with comparable preclinical oral efficacy to **2** but with improved canine oral bioavailability (Fig. 1).

In previously published work on the chlorofluorophenylacetamide P2 scaffold¹⁰ typified by **4** (Fig. 2), the fluorine atom proved to be a competent hydrogen-bond acceptor isosteric with the carbonyl oxygen of the pyridinone¹¹ and pyrazinone¹² (e.g., **3**) P2 scaffolds, as evidenced by the F–H–N heteroatom distance of 3.17 \AA .¹⁰

However, numerous examples of the chlorofluorophenylacetamide series suffered from poor dog pharmacodynamic parameters¹³ perhaps because of relatively high plasma protein binding, and required multistep functional group manipulation for P3 installation.¹⁰ It was hypothesized that replacement of the chloro moiety with a cyano group⁶ would increase the polarity for the series, thereby potentially reducing plasma protein binding, while allowing for a shorter, higher-yielding synthetic route to targets. As expected, **5** was not only more polar

and slightly less plasma protein-bound than **4**, it was also significantly more potent in vitro (Table 1).

The synthesis of **5** is described in Scheme 1. Reaction of sodium diethyl malonate with trifluorobenzonitrile **6**, followed by Krapcho decarboxylation, afforded a 1.35:1 mixture of regioisomers that were separated by flash chromatography to afford key P2 intermediate **7** as the minor regioisomer in 34% overall yield. Fluorinated P3 amines **10** were accessed via reaction of a (hetero)aryl halide **8** with ethyl bromodifluoroacetate and copper bronze with activated esters **9**.¹⁴ The phenyl-derived amines **10** were then efficiently obtained via treatment of **9** with ammonia followed by borane reduction of the amide. Since borane overreacted with the analogous pyridyl-derived amides, pyridyl-derived esters **9** (A = N) were reduced to the alcohol, converted to the azide in two steps, and cleanly hydrogenated to the amines **10** with palladium on carbon. The P3–P2 linkage was established by a straightforward S_NAr reaction between P3 amines **10** and P2 electrophile **7**. Subsequent saponification, amide bond formation with a P1 amine (e.g., oxyguanidine-containing **13**), and, if necessary, Boc deprotection, afforded final targets such as **5**. The P1 amine **13** was obtained in a four-step sequence



Scheme 1. Reagents and conditions: (a) NaH (2.2 mol equiv), diethyl malonate (2.2 mol equiv), THF, rt, 4 d, 98% (1.35:1 regioisomers); (b) LiCl (1 mol equiv), water (1.3 mol equiv), DMSO, 120 °C, 40 min, 35% (desired regioisomer); (c) for A = CH, X = I or A = N, X = Br: Cu bronze (2.2 mol equiv), ethyl bromodifluoroacetate (1.2 mol equiv), DMSO, rt, 3 d, 56–97%; (d) for A = CH; i—NH₃, MeOH, rt, 13 h, 95%; ii—borane, THF, reflux, 9 h, 67% after acid workup; (e) for A = N; i—NaBH₄, EtOH, 0 °C, 3 h, 100%; ii—I₂, imidazole, PPh₃, toluene/MeCN (2:1), 0 °C → 90 °C, 33%; iii—NaN₃, DMSO, 90 °C, 2 d, 93%; iv—H₂ (balloon), EtOAc, 10% Pd/C, 24 h, 86%; (f) **7** (1.25 mol equiv), (*i*-Pr)₂NEt (1.3 mol equiv), DMSO, 110 °C, 3 d, 64%; (g) 1 M LiOH (aq)/MeOH/THF (1:1:2), 50 °C, 1 h, 100%; (h) i—**13** (1.2 mol equiv), BOP, (*i*-Pr)₂NEt, CH₂Cl₂/MeCN (1:1), rt, 8 h, 83%; ii—CH₂Cl₂/CF₃CO₂H/anisole (3:1:0.4, v/v), rt, 10 h, 84%; (i) *N*-hydroxyphthalimide, PPh₃, (CO₂Et)N=N(CO₂Et), THF, rt, o/n, 91%; (j) 40% MeNH₂, THF/EtOH (1:1), rt, 1 h, 95%; (k) *N,N'*-bis-Boc-1-guanylpyrazole, DMF, rt, o/n, 93%; (l) H₂ (balloon), 10% Pd/C, THF/EtOH (1:1), rt, 30 min, 61%.

Table 1. In vitro potency, plasma protein binding, and $2 \times$ aPTT values for compounds **1–5** using human thrombin and plasma

Compound	K_i thrombin (nM)	Plasma protein binding (%)	clogP	$2 \times$ aPTT (μM)
1 ^a	4	>98	2.98	7.9
2 ^b	4	45.7	−1.35	0.23
3 ^c	0.1	—	1.52	0.29
4	47	95 ^d	3.04	—
5	2.3	92.6 ^d	2.52	0.64

^a Ref. 7.

^b Ref. 9.

^c Ref. 12.

^d Dog plasma protein binding.

Table 2. P3 structure–activity relationships


Compound	R	A	K_i (nM)	Trypsin ratio ^a	$2 \times$ aPTT ^b (μ M)	PPB ^b (%)	Caco ^c	Dog PD ^d	
								t (h) $\geq 2 \times$ aPTT ^e	Fold aPTT max ^f
5	H	CH	2.3	478	0.64	93.7	1.1, 4.6	—	—
14	H	N	1.2	1170	0.36	56	0.9, 8.5	5	2.83
15	6-Me	N	10	770	—	—	—	—	—
16	5-Me	N	2.9	148	0.43	—	—	—	—
17	4-Me	N	1.2	4080	0.41	97.6	0.2, 2.1	3.5	2.88
18	3-Me	N	0.79	1110	0.22	—	—	4.5	2.38
19	4-Cl	N	0.57	6840	—	—	—	5.5	2.51
20	P3 = 8-quinolyl		0.38	1580	0.44	99.6	1.7, —	0	1.23
21	3-Cl	CH	1.7	760	0.76	95.2	0.8, 9.9	0	1.87
22	3-F	CH	3.2	750	0.59	85	0.7, 4.7	—	—
23	3,4-diF	CH	1.8	2000	0.68	99.0	0.5, 2.6	0	1.67
24	6-SO ₂ Me	CH	0.65	1850	—	—	—	0	1.04
25	H	<i>N</i> -Oxide	1.3	770	—	—	—	0	1.89
26	4-Cl	<i>N</i> -Oxide	0.66	5300	—	—	—	0	1.20

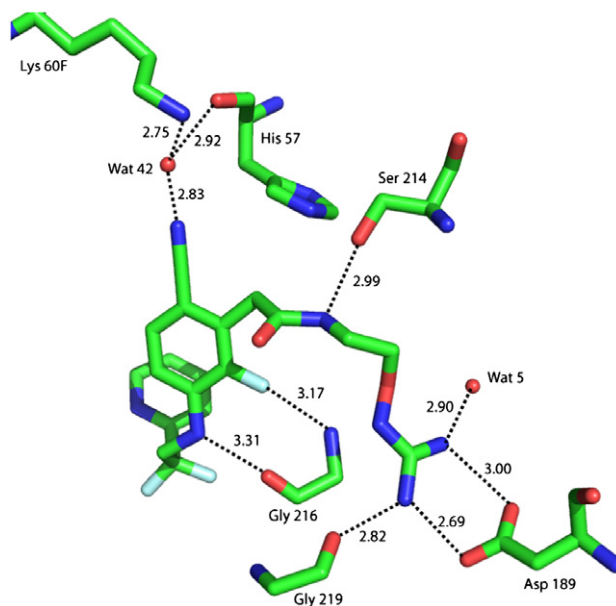
^a K_i trypsin/ K_i thrombin.^b In vitro assay using human plasma.^c A \rightarrow B, B \rightarrow A; P_{app} in 10^{-6} cm/s.^d Single 10 mg/kg oral dose in 2–5 dogs.^e Number of hours that the aPTT is $\geq 2 \times$ the baseline value over the course of 8 h post-dose (7 time points).^f Peak aPTT multiple of baseline seen over 8 h.

from alcohol **11** in 49% overall yield, with the final step requiring careful hydrogenolysis of the Cbz group to avoid N–O bond cleavage.

Building upon the P3 SAR generated from the chloro-fluorophenylacetamide series,¹⁰ it was discovered that the 2-pyridyl analogue **14** provided a roughly 2-fold improvement in human thrombin potency, $2 \times$ aPTT value, and trypsin selectivity compared to phenyl analogue **5** (Table 2). In addition, **14** had significantly decreased plasma protein binding compared to **5**, in line with its reduced clog P value of 1.61. However, neither **5** nor **14** had robust permeability as measured by apical to basolateral transfer (A \rightarrow B) across a Caco cell monolayer ($P_{app} = 1.1$ and 0.9×10^{-6} cm/s, respectively), and indeed, **14** demonstrated increased efflux as indicated by the Caco B \rightarrow A/A \rightarrow B ratio of 9.7 (compared to 4.7 for **5**). This was of potential concern, since Caco permeability had correlated with bioavailability for several other thrombin inhibitor series, including those represented by **1** and **2** (1 A \rightarrow B $P_{app} = 4.1 \times 10^{-6}$ cm/s, with rat $F = 24\%$ and 2 A \rightarrow B $P_{app} = 0.7 \times 10^{-6}$ cm/s, with rat $F = 6\%$).

In an attempt to improve the in vitro parameters of **14**, particularly Caco permeability, methyl substitution on the pyridyl P3 moiety was explored. Analogues **17** and **18** proved to be potent and selective with $2 \times$ aPTT values comparable to that seen for **14**. However, methyl substitution significantly increased plasma protein binding while showing no improvement in Caco permeability (**17**, Table 2). Attempts were made to enhance the selectivity and permeability of the phenyl analogue **5** with

halogenated derivatives **21–23**. However, while selectivity increased for these analogues, Caco permeability became somewhat worse. Finally, polar electron-withdrawing substituents at the ortho position of the P3 (hetero)aromatic ring were found to confer potency (**24–26**) as expected.¹⁵ By contrast, modestly potent **15** may not be able to satisfy a binding mode seen in previous thrombin co-crystal structures whereby the ortho polar moiety (e.g., *N,N*-oxide) faces solvent,¹⁵ with

**Figure 3.** Crystal structure of **14** bound to thrombin (PDB ID:2C27).

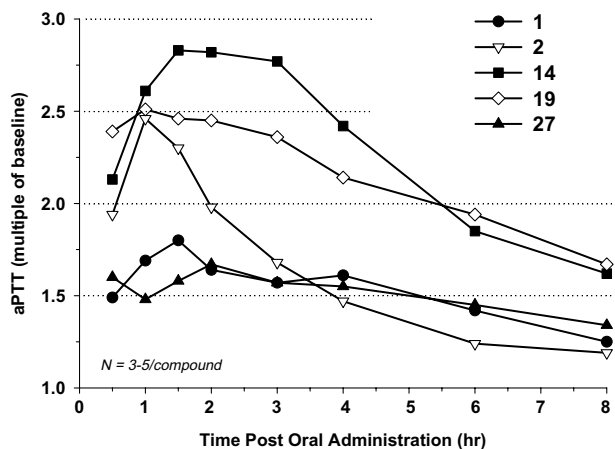


Figure 4. aPTT following a single 10 mg/kg oral dose to conscious dogs.

the ortho hydrogen found in **24–26** (but not **15**) accessing a favorable $\sigma-\pi$ interaction with Trp215.^{10,15}

The X-ray crystal structure of **14** bound to human thrombin is shown in Figure 3. As in previous structures, the oxyguanidine P1–S1 hydrogen-bonding network is intact,¹⁰ and the hydrogen bonds with Gly216 and Ser214 are also maintained.^{6,10,15} However, the nitrile nitrogen of **14** additionally forms a 2.8 Å hydrogen bond with a water molecule that in turn forms H-bonds with Lys60F (2.8 Å) and His57 (2.9 Å). This nitrile-based H-bonding network may account in part for the increased potency of the cyanofluorophenylacetamides versus chlorofluorophenylacetamides.

Since a sampling of the compounds in Table 2 showed good stability (69–100% remaining after a 10 min incubation with human and dog microsomes at 37 °C; four examples), 10 of the analogues were profiled in an oral dog pharmacodynamic (PD) assay (Fig. 4). Notably, **14**, **17**, and **19** demonstrated a ≥ 2.5 -fold increase in aPTT for at least 3 h following a single 10 mg/kg oral dose (Table 2). This degree of anticoagulation is superior to that shown by **1**, and indeed to that seen for **2** (Fig. 4). Interestingly, chlorofluorophenylacetamide **27** ($K_i = 1.8$ nM; $\text{clog}P = 2.69$), the chloro congener of **19** ($K_i = 0.6$ nM; $\text{clog}P = 2.16$), was significantly less active than **19** (Fig. 4).

In general, improvements in canine PD in this series correlate with lower in vitro $2 \times$ aPTT values and lower plasma protein binding (or lower $\text{clog}P$). However, the presence of additional polar heteroatoms (e.g., **24–26**) had a detrimental effect on PD, perhaps due to an unacceptable loss of permeability.

Since **14** had robust PD as well as an attractive in vitro profile across species (e.g., $\geq 86\%$ remaining after 10 min incubation with human, dog, or rat microsomes; $\leq 69\%$ PPB in human, dog, or rat plasma), it was screened for off-target binding and cardiovascular safety. Compound **14** showed little effect against a Cerep panel of 50 receptors, ion channels, and transporters ($<40\%$ inhibition at 10 μM), and was notably clean in

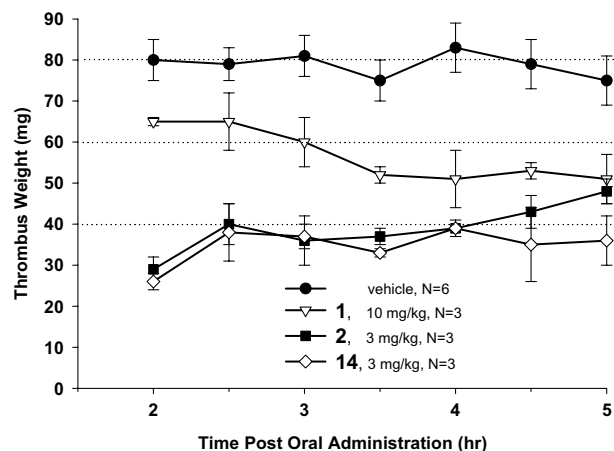


Figure 5. Oral antithrombotic efficacy of **1**, **2**, and **14** in the A-V shunt model in anesthetized dogs.

a hERG ion channel patch-clamp study compared to **1** (0% inh. vs 85% inh. at 10 μM , respectively). In addition, **14** caused no significant heart rate-corrected QT interval prolongation in guinea pigs up to 10 mg/kg iv (data not shown).

Therefore, the efficacy of **14** was explored in a dog arteriovenous (A-V) shunt model¹⁶ (Fig. 5) and a rat electrically stimulated carotid artery (ESCA) model¹⁷ (Fig. 6). Compound **14** inhibited thrombus formation by 67–51% for at least 5 h following a 3 mg/kg oral dose in dogs (Fig. 5). This is comparable to the antithrombotic effect of **2**, and is superior to that for **1**. The rat intravenous data mirrored this trend: **14** (iv $\text{ED}_{50} \sim 40$ $\mu\text{g}/\text{kg}$) and **2** have comparable efficacy, and both are substantially superior to **1** as well as to the marketed iv antithrombotic argatroban (Fig. 6).

The PK parameters of several analogues are listed in Table 3. The dog PK of **14**, **17**, and **18** support the dog PD described in Table 2. All three have oral half-lives greater than 2 h, with C_{max} values at least 7-fold higher than the concentrations needed to double the activated partial thromboplastin times of (human) plasma in vitro.

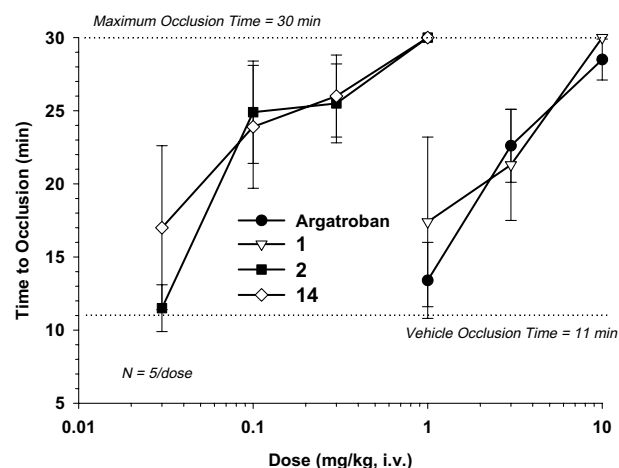


Figure 6. Intravenous antithrombotic efficacy of **1**, **2**, and **14** relative to argatroban in the ESCA rat model.

Table 3. Dog, rat, and monkey PK of select analogues

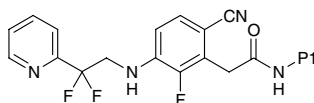
Compound	Species ^a	C_{\max} po (μM)	$t_{1/2}$ po (h)	$t_{1/2}$ iv (h)	Cl ^b (mL/min/kg)	Vd _{ss} ^c (L/kg)	F (%)
14	Dog	3.5	2.5	2.9	13 (42%)	2.9	49
17	Dog	2.8	2.5	3.6	18 (58%)	3.6	45
18	Dog	3.3	3.2	2.8	15 (49%)	2.9	65
14	Rat ^d	0.03	—	1.0	67 (122%)	~6	2
17	Rat	0.25	2.5	1.3	30 (55%)	2.3	2

^a Unless otherwise noted: dog 10 mg/kg, po, 1 mg/kg, iv; rat 30 mg/kg, po, 3 mg/kg, iv.

^b Clearance (as a percentage of liver blood flow in parentheses).

^c Volume of distribution at steady state. Both clearance and Vd determined from iv dosing.

^d 10 mg/kg, po, 2 mg/kg, iv.

Table 4. P1 structure–activity relationships

Compound	P1	K_i (nM)	Trypsin ratio ^a	PPB ^b (%)	Caco ^c
34		9	640	—	0.6, 0.3
35		11	400	85	—
36		0.77	2000	89	3.9, 13
37		33	>300	—	—
38		19	>500	98.7	—

^a K_i trypsin/ K_i thrombin.

^b In vitro assay using human plasma.

^c A \rightarrow B, B \rightarrow A; P_{app} in 10^{-6} cm/s.

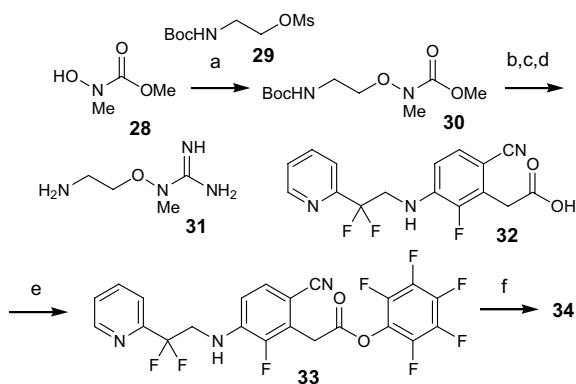
In addition, the dog bioavailabilities ranged from 45% to 65%, an improvement over that observed for **2** (24%).⁹ However, **14** and **17** had unacceptably low bioavailability in rats (2%) despite excellent rat microsomal stability (>95% remaining after a 10 min incubation), and the less polar analogues **21** and **23** had only marginally better rat bioavailability. In addition, clearance sometimes exceeded hepatic blood flow, indicating the possibility of extrahepatic metabolism in the rat.¹⁸

In order to ascertain whether the poor rat bioavailability of **14** was caused by poor permeability across the intestinal mucosa, or by metabolism upon first pass through the liver, rats were dosed orally at 10 mg/kg and blood samples from the portal vein (pre-liver) and jugular vein (post-liver) were collected over 6 h. Neither sample site contained significant amounts of **14**, indicating that **14** had little propensity for diffusion across the small intestine into the portal vein. Dosing **14** by cannula directly

into the ascending colon also yielded ~2% bioavailability as with oral dosing, indicating that the molecule is not colonically absorbed (data not shown).

Since increased hydrogen-bond donor count was found to correlate with decreased Caco permeability across thrombin chemical series within this discovery program, oxyguanidine was replaced with P1s containing fewer H-bond donors (Table 4). The synthesis of *N*-methyl-oxyguanidine P1 **31** found in **34** is described in Scheme 2, while the P1 moieties in **35–38** were previously reported.^{6,12,19}

Unfortunately, **34** provided no improvement in Caco A \rightarrow B permeability, and potency dropped 7-fold relative to **14**. Methylation at the distal oxyguanidine nitrogen had dramatically reduced thrombin potency in another thrombin series (data not shown) and so was not explored here. Compounds **35**, **37**, and **38** also



Scheme 2. Reagents and conditions: (a) NaH (0.94 mol equiv), **29** (0.77 mol equiv), DMF, 0 °C → rt, 6%; (b) KOH (2.6 mol equiv), water, 90 °C, 18 h, 85%; (c) *N,N'*-bis-Boc-1-guanylpyrazole, DMF, 50 °C, o/n, 63%; (d) 12 N HCl (aq), rt, 30 min, 100%; (e) pentafluorophenol (3 mol equiv), (*i*-Pr)₂N=N(*i*-Pr) (2 mol equiv), DMF, CH₂Cl₂, rt, 24 h, 50%; (f) **31**, DMF, (*i*-Pr)₂NEt (4 mol equiv), rt, 12 h, 75%.

lacked sufficient potency for further profiling. Compound **36** was potent and selective, with reasonable PPB and improved Caco permeability (Table 4). Unfortunately, its dog PK profile (oral C_{max} = 0.8 μM; iv $t_{1/2}$ = 1.1 h; Cl = 34 mL/min/kg; 26% *F* at 10 mg/kg, po, 1 mg/kg, iv) was inferior in all respects to that for **14**, and it was inactive in the oral dog PD assay (aPTT maximum multiple of baseline = 1.3, compared to 2.8 for **14**). Perhaps phase II conjugation of the amino group⁶ was responsible for the poor PK of **36**, since it had excellent dog microsomal stability (100% remaining after 10 min at 37 °C).

In conclusion, the novel 2-cyano-6-fluorophenylacetamide P2 scaffold, after suitable optimization of the P1 and P3 moieties, can provide potent thrombin inhibitors. Thus, we obtained **14**, as a potent thrombin inhibitor with robust dog PK and efficacy. However, within this series of thrombin inhibitors, acceptable rat bioavailability proved elusive.

References and notes

- Rosamond, W.; Flegal, J.; Friday, G.; Furie, K.; Go, A.; Greenlund, K.; Haase, N.; Ho, M.; Howard, V.; Kissela, B.; Kittner, S.; Lloyd-Jones, D.; McDermott, M.; Meigs, J.; Moy, C.; Nichol, G.; O'Donnell, C. J.; Roger, V.; Rumsfeld, J.; Sorlie, P.; Steinberger, T. T.; Wasserthiel-Smoller, S.; Hong, Y. *Circulation* **2007**, *115*, 69.
- Ali, S.; Hong, M.; Antezano, E. S.; Mangat, I. *Cardiovasc. Hematol. Disord. Drug Targets* **2006**, *6*, 233.
- Masic, L. P. *Curr. Med. Chem.* **2006**, *13*, 3627.
- Gustafsson, D.; Nystrom, J.; Carlsson, S.; Bredberg, U.; Eriksson, U.; Gyzander, E.; Elg, M.; Antonsson, T.; Hoffmann, K.; Ungell, A.; Sorensen, H.; Nagard, S.; Abrahamsson, A.; Bylund, R. *Thromb. Res.* **2001**, *101*, 171.
- Hauel, N. H.; Nar, H.; Priepeke, H.; Ries, U.; Stassen, J.-M.; Wiene, W. *J. Med. Chem.* **2002**, *45*, 1757.
- Burgey, C. S.; Robinson, K. A.; Lyle, T. A.; Sanderson, P. E. J.; Lewis, S. D.; Lucas, B. J.; Krueger, J. A.; Singh, R.; Miller-Stein, C.; White, R. B.; Wong, B.; Lyle, E. A.; Williams, P. D.; Coburn, C. A.; Dorsey, B. D.; Barrow, J. C.; Stranieri, M. T.; Holahan, M. A.; Sitko, G. R.; Cook, J. J.; McMasters, D. R.; McDonough, C. M.; Sanders, W. M.; Wallace, A. A.; Clayton, F. C.; Bohn, D.; Leonard, Y. M.; Detwiler, T. J., Jr.; Lynch, J. J., Jr.; Yan, Y.; Chen, Z.; Kuo, L.; Gardell, S. J.; Shafer, J. A.; Vacca, J. P. *J. Med. Chem.* **2003**, *46*, 461.
- Lu, T.; Markotan, T.; Coppo, F.; Tomczuk, B.; Crysler, C.; Eisennagel, S.; Spurlino, J.; Gremminger, L.; Soll, R. M.; Giardino, E. C.; Bone, R. *Bioorg. Med. Chem. Lett.* **2004**, *14*, 3727.
- Langdell, R. D.; Wagner, R. H.; Brinkhous, K. M. *J. Lab. Clin. Med.* **1953**, *41*, 637.
- Maryanoff, B. E.; McComsey, D. F.; Costanzo, M. J.; Yabut, S. C.; Lu, T.; Player, M. R.; Giardino, E. C.; Damiano, B. P. *Chem. Biol. Drug Des.* **2006**, *68*, 29.
- Lee, L.; Kreutter, K. D.; Pan, W.; Crysler, C.; Spurlino, J.; Player, M. R.; Tomczuk, B.; Lu, T. *Bioorg. Med. Chem. Lett.* **2007**, *17*, 6266.
- Tamura, S. Y.; Semple, J. E.; Reiner, J. E.; Goldman, E. A.; Brunck, T. K.; Lim-Wilby, M. S.; Carpenter, S. H.; Rote, W. E.; Oldeshulte, G. L.; Richard, B. M.; Nutt, R. F.; Ripka, W. C. *Bioorg. Med. Chem. Lett.* **1997**, *7*, 1543.
- Sanderson, P. E. J.; Lyle, T. A.; Cutrona, K. J.; Dyer, D. L.; Dorsey, B. D.; McDonough, C. M.; Naylor-Olsen, A. M.; Chen, I.-W.; Chen, Z.; Cook, J. J.; Cooper, C. M.; Gardell, S. J.; Hare, T. R.; Krueger, J. A.; Lewis, S. D.; Lin, J. H.; Lucas, B. J., Jr.; Lyle, E. A.; Lynch, J. J.; Stranieri, M. T.; Vastag, K.; Yan, Y.; Shafer, J. A.; Vacca, J. P. *J. Med. Chem.* **1998**, *41*, 4466.
- Table 2^{e,f}.
- Eto, H.; Kaneko, Y.; Sakamoto, T. *Chem. Pharm. Bull.* **2000**, *48*, 982.
- Burgey, C. S.; Robinson, K. A.; Lyle, T. A.; Nantermet, P. G.; Selnick, H. G.; Isaacs, R. C. A.; Lewis, S. D.; Lucas, B. J.; Krueger, J. A.; Singh, R.; Miller-Stein, C.; White, R. B.; Wong, B.; Lyle, E. A.; Stranieri, M. T.; Cook, J. J.; McMasters, D. R.; Pellicore, J. M.; Pal, S.; Wallace, A. A.; Clayton, F. C.; Bohn, D.; Welsh, D. C.; Lynch, J. J.; Yan, Y.; Chen, Z.; Kuo, L.; Gardell, S. J.; Shafer, J. A.; Vacca, J. P. *Bioorg. Med. Chem. Lett.* **2003**, *13*, 1353.
- Sklar, A. H.; Bond, G. C.; Lightfoot, B.; Fowler, B.; Ginsburg, J. *J. Lab. Clin. Med.* **1988**, *111*, 537.
- Charlton, P. A.; Faint, R. W.; Bent, F.; Bryans, J.; Chicarelli-Robinson, I.; Mackie, I.; Machin, S.; Bevan, P. *Thromb. Haemost.* **1996**, *75*, 808.
- Krishna, D. R.; Klotz, U. *Clin. Pharmacokinet.* **1994**, *26*, 144.
- Lepore, S. D.; Wiley, M. R. *J. Org. Chem.* **2000**, *65*, 2924.